Correlations of Solution Rheology with Electrospun Fiber Formation of Linear and Branched Polyesters

Matthew G. McKee,[†] Garth L. Wilkes,[‡] Ralph. H. Colby,[§] and Timothy E. Long*[,†]

Department of Chemistry and Department of Chemical Engineering, Virginia Tech, Blacksburg, Virginia 24061, and Department of Materials Science and Engineering, The Pennsylvania State University, University Park, Pennsylvania 16802

Received November 10, 2003; Revised Manuscript Received December 15, 2003

ABSTRACT: The implications of the entanglement concentration (C_e) on the electrospinning process for a series of linear and branched poly(ethylene terephthalate-*co*-ethylene isophthalate) (PET-*co*-PEI) copolymers with weight-average molecular weights (M_w) ranging from 11 700 to 106 000 g/mol and branching index values (g') from 1.0 to 0.43 were investigated. Analyzing the dependence of specific viscosity (η_{sp}) on concentration enabled the determination of the semidilute unentangled, semidilute entangled, and concentrated regimes for the PET-*co*-PEI solutions. Linear and branched copolymers were electrospun from semidilute unentangled, semidilute entangled, and concentrated solutions under identical conditions to determine the effects of concentration regime and molecular topology on electrospun fiber morphology. The dependence of the fiber diameter and morphology on the zero shear rate viscosity (η_0) and normalized concentration (C/C_e) was determined. For copolyesters with molecular weights well above the entanglement molecular weight, C_e was the minimum concentration required for electrospinning of beaded fibers, while 2−2.5 times C_e was the minimum concentration required for electrospinning of uniform, bead-free fibers. When the concentration was normalized with C_e, the influence of chain length and topology on the electrospinning process was removed, and the fiber diameter universally scaled with the normalized concentration to the 2.6 power.

1. Introduction

Traditionally, polymer fibers are spun using pressure-driven flow through an extruder, which yield fibers on the order of 10−100 μm in diameter. The electrospinning process utilizes an electrostatic potential to create submicron size fibers on the order of 100 nm in diameter.[1,2] Electrospinning occurs when a charged polymer solution or melt, possessing sufficient molecular entanglements, emits a charged fluid jet in the presence of an electric field. The charged jet follows a chaotic trajectory of stretching and splaying until it reaches its grounded target, thereby completing the circuit. A charged droplet of solution suspended at the end of a capillary deforms into a conical shape, or Taylor cone, when subjected to a Coulumbic force.[3] The Taylor cone is formed due to a balancing of the repulsive nature of the charge distribution on the droplet's surface and the surface tension of the liquid.[4] As the charge is increased above a critical voltage, a stable jet is discharged from the tip of the Taylor cone.

A jet of low molecular weight fluid breaks up into small droplets, a phenomenon termed electrospraying, while a polymer solution with sufficient chain overlap and entanglements does not break up but undergoes a bending instability that causes a whiplike motion between the capillary tip and the grounded target.[5] Researchers investigated the instabilities of the electrically forced jet and developed a model that relates the dependence of the bending instability on the electric field and solution flow rate.[6] It is this bending instability that accounts for the high degree of single fiber drawing, which results in submicron size fibers. The small fiber size and disordered deposition onto the grounded target yield nonwoven, three-dimensional, fiber mats with a high specific surface area and a submicron degree of porosity.[7] The unique fibers are suitable as filtration devices, membranes, vascular grafts, protective clothing, and tissue scaffolding applications.[8−10] Recently, simultaneous electrospinning of two polymer solutions yielded bicomponent submicron fibers that possessed properties of each of the polymer components.[11]

The effects of processing variables including applied voltage, tip to target distance, and the feed rate of the solution to the capillary tip and solution properties like solvent, viscosity, concentration, conductivity, and surface tension on electrospun fiber morphology were extensively investigated for a variety of polymeric systems.[1,12,13] It has been shown for many polymer/solvent systems that increasing the solution concentration or viscosity decreases the number of bead defects and increases the overall fiber diameter of the electrospun fibers.[14] Moreover, researchers have electrospun polymer solutions with varying concentration resulting in viscosities that ranged over an order of magnitude and reported the resulting fiber structure.[15,16] However, more detailed investigations of the dependence of fiber morphology on solution rheological behavior in the literature are not reported. For instance, the influence of the chain overlap concentration (C^*) or the entanglement concentration (C_e) for a given polymer/solvent system on the electrospinning process is lacking.

Colby et al. measured the concentration dependence of viscosity of linear polymers in good solvents and identified four different concentration regimes including the dilute, semidilute unentangled, semidilute entangled, and concentrated regimes.[17,18] The entanglement concentration, C_e, is the boundary between the semidilute unentangled and semidilute entangled regimes and is defined as the point at which significant

* To whom correspondence should be addressed.
[†] Department of Chemistry, Virginia Tech.
[‡] Department of Chemical Engineering, Virginia Tech.
[§] Pennsylvania State University.

10.1021/ma035689h CCC: $27.50
Published on Web 02/06/2004

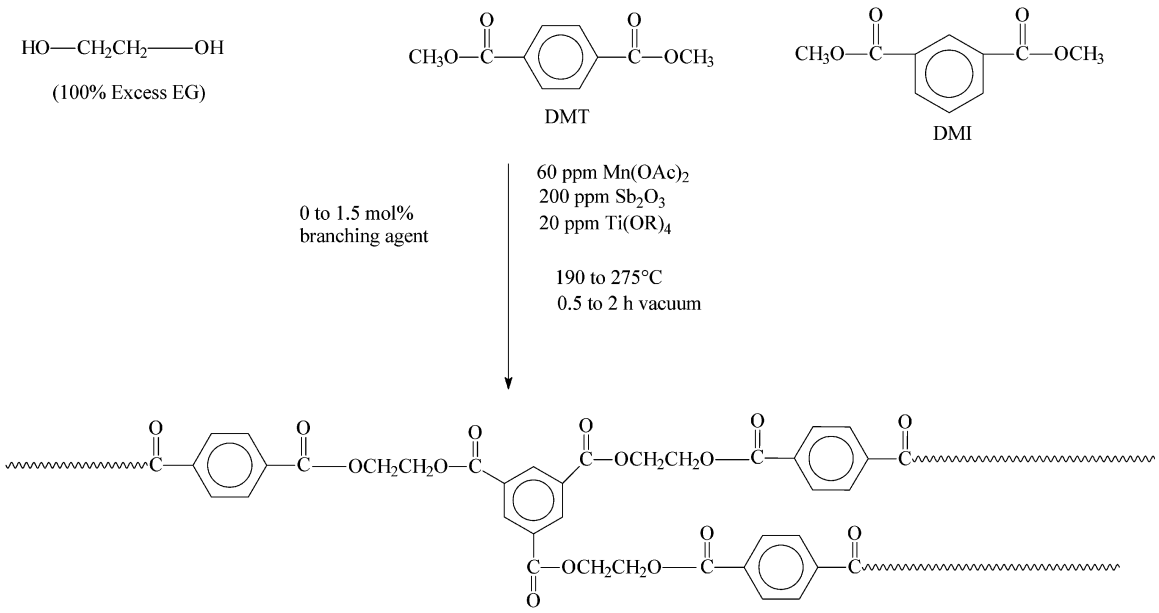

Figure 1. Synthesis of branched PET-*co*-PEI copolymers.

overlap of the polymer chains topologically constrain the chain motion, causing entanglement couplings.[19] Because of their higher segment density, branched polymers possess a smaller hydrodynamic volume than linear polymers of equivalent molecular weight and consequently have a larger C_e compared to those of linear chains.[20] As concentration is increased into the concentrated regime (C^{**}), polymer chain entanglements dominate the flow behavior, and the chain dimensions become independent of concentration.[19]

Our objective is to identify the semidilute entangled concentration regime for a series of linear and randomly branched, partially aromatic polyesters and to determine the influence of C_e on the electrospinning process. Herein, empirical relationships of solution rheology and electrospun fiber formation for a series of linear and branched poly(ethylene terephthalate-*co*-ethylene isophthalate) (PET-*co*-PEI) copolymers are presented. The synthesis of branched and functional polyesters has received significant attention in our laboratories.[21−23]

2. Experimental Section

2.1. Materials. Dimethyl terephthalate (DMT), dimethyl isophthalate (DMI), ethylene glycol, trimellitic anhydride (TMA), 1,3,5-trimethylbenzene tricarboxylate (1,3,5-TMT), and 1,2,4-trimethylbenzene tricarboxylate (1,2,4-TMT) were purchased from the Aldrich Chemical Co. Chloroform ($CHCl_3$) and dimethylformamide (DMF) were purchased from VWR. All reagents and solvents were used as received without further purification.

2.2. Electrospinning Schematic. The polyesters were dissolved in a 70/30 w/w mixture of $CHCl_3$/DMF at various concentrations and placed in a 20 mL syringe, which was mounted in a syringe pump (KD Scientific Inc, New Hope, PA). The positive lead of a high-voltage power supply (Spellman CZE1000R; Spellman High Voltage Electronics Corp.) was connected to the 18 gauge needle of the syringe via an alligator clip. A grounded, metal target (304 stainless steel mesh screen) was placed 24 cm from the tip of the syringe needle. The syringe pump delivered the polymer solution at a controlled flow rate of 3 mL/h, while the voltage was kept constant at 18 kV.

2.3. Characterization. Molecular weights were determined at 40 °C in chloroform (HPLC grade) at 1 mL min^{-1} using polystyrene standards on a Waters GPC equipped with three in-line PLgel 5 mm Mixed-C columns with an autosampler, a 410 RI detector, a Viscotek 270 dual detector, and an in-line Wyatt Technologies miniDawn multiple angle laser light scattering (MALLS) detector. All samples were dissolved in $CHCl_3$ and analyzed at 40 °C. ^{1}H NMR spectroscopy was performed on a Varian Unity 400 spectrometer at 400 MHz in $CDCl_3$. Solution rheology was performed with a VOR Bohlin strain-controlled solution rheometer at 25 ± 0.2 °C using a concentric cylinder geometry. Differential scanning calorimetry (DSC) was performed with a Perkin-Elmer Pyris 1 DSC at a heating rate of 10 °C min^{-1} after quenching from 290 °C at room temperature under nitrogen. Electrospun fiber diameter and morphology were analyzed using a Leo 1550 field emission scanning electron microscope (FESEM). Fibers for FESEM analysis were collected on a $^1/_4$ in. × $^1/_4$ in. stainless steel mesh, mounted onto an SEM disk, and sputter-coated with a 8 nm Pt/Au layer to reduce electron charging effects.

2.4. Synthesis of Poly(ethylene terephthalate-*co*-ethylene isophthalate). An equimolar mixture of DMT and DMI and 100% excess ethylene glycol were added to a 250 mL round-bottom flask equipped with a mechanical agitator. 1,3,5-TMT, 1,2,4-TMT or TMA (0−3.0 mol %), and the catalyst system (200 ppm of Sb_2O_3, 20 ppm of $Ti(OR)_4$, and 60 ppm of $Mn(OAc)_2$) were added to the round-bottom flask. The reaction proceeded under a nitrogen atmosphere, and the temperature was raised from 190 to 220 to 275 °C in 2 h increments. Vacuum (0.1−0.2 mmHg) was then initiated for 0.5−2 h at 275 °C. The product polymer was characterized using ^{1}H NMR spectroscopy without further purification. No low molecular weight cyclics were observed in the GPC traces.

3. Results and Discussion

3.1. Synthesis and Characterization of Randomly Branched PET-*co*-PEI. A reaction scheme for the PET-*co*-PEI synthesis is shown in Figure 1. DMT and DMI were reacted with ethylene glycol to form bis(hydroxyethyl) terephthalate which undergoes polycondensation to produce a high molecular weight polyester as ethylene glycol is removed under vacuum. DMT and DMI were selected as comonomers due to the respective para and meta substitution which disrupts the resulting polymer chain symmetry, thereby reducing the level of crystallinity and increasing polymer solubility for subsequent electrospinning studies.

Differential scanning calorimetry (DSC) revealed that the linear and branched PET-*co*-PEI copolymers were completely amorphous with a glass transition temper-

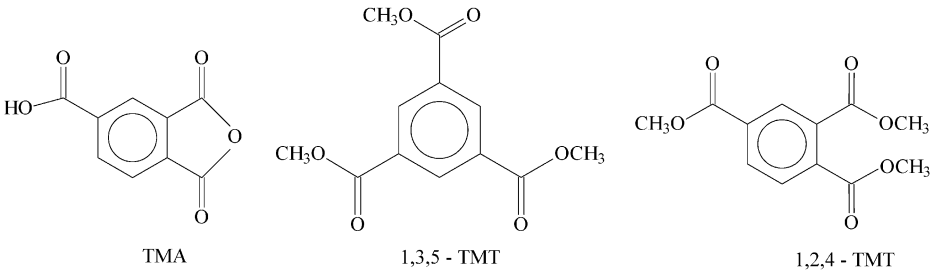

Figure 2. Branching agents utilized in PET-*co*-PEI step growth polymerization.

Table 1. Reaction Conditions and Molecular Weight Data for Linear and Branched PET-*co*-PEI

branching agent	branching agent concn (mol %)	vacuum time (h)	M_w (kg/mol)	M_w/M_n
N/A[a]	0	0.5	11.7	1.6
	0	1.0	54.2	1.6
	0	2.0	77.3	1.6
1,3,5-TMT	0.5	0.5	49.2	3.7
	0.5	1.0	86.5	3.0
	0.5	1.5	12 wt % gel	
	1.0	0.5	94.0	3.6
	1.5	0.5	30 wt % gel	
TMA	0.5	0.3	30.0	2.3
	0.5	0.5	92.5	2.9
	0.5	1.0	130	3.4
	0.5	1.5	56 wt % gel	
	1.0	0.5	176	6.6
	1.5	0.5	>99 wt % gel	
1,2,4-TMT	0.5	0.5	60.0	2.2
	0.5	1.0	106	2.5

[a] N/A = not applicable.

ature (T_g) at approximately 68 °C. This is expected as the meta substitution of the dimethyl isophthalate disrupts the chain symmetry and prevents chain folding. Moreover, the glass transition was independent of the degree of branching, as the T_g did not vary from 68 °C for any of the samples. This phenomenon has been reported previously for randomly branched PET.[24]

^{1}H NMR spectroscopy revealed that all the linear and branched copolymers inherently contained 2−3 mol % of diethylene glycol (DEG) units due to self-condensation of ethylene glycol. Under these reaction conditions, this composition of DEG is consistent with the prior literature.[25] Unfortunately, the branching composition could not be determined using ^{1}H NMR spectroscopy since the peak integrations for the protons associated with the branching unit were convoluted with the aromatic protons in the polyester backbone. Figure 2 shows the structures of the three different branching agents employed in the polycondensation reactions. 1,3,5-TMT and 1,2,4-TMT are trimethyl esters that only differ in substitution of the phenyl group. TMA is also a trifunctional branching agent that undergoes anhydride ring opening during the step growth reaction.

Because of the statistical nature of the branching reaction, the polyester weight-average molecular weight (M_w) and polydispersity (M_w/M_n) increased as the incorporation of branching agent was increased. To investigate the influence of branching on the electrospinning process, it is imperative that the linear and branched copolymers have the same M_w to deconvolute the effects of molecular weight and branching. Consequently, the polycondensation reaction time was reduced in the presence of a branching agent. Table 1 lists the copolyesters that were synthesized and the corresponding polycondensation reaction times and molecular weight data. It is important to note that the final vacuum was 0.2 mmHg.

At 0.5 h vacuum time, increasing the concentration of 1,3,5-TMT branching agent from 0 to 1.0 mol % increased the M_w from 11 700 to 94 000 g/mol and broadened the molecular weight distribution from 1.8 to 3.6. Moreover, increasing the 1,3,5-TMT branching content further to 1.5 mol % produced PET-*co*-PEI with a significant gel content (30 wt % gel). To match molecular weights for the linear and branched polyesters, the vacuum time was reduced to decrease the conversion of the branched macromolecules. Table 1 illustrates approximately equivalent M_w were obtained for the linear (54 200 g/mol) and 0.5 mol % branched PET-*co*-PEI using 1,3,5-TMT and 1,2,4-TMT (49 200 and 60 000 g/mol, respectively) when the reaction time for the branched polyester was 50% of the reaction time for the linear polyester. Other researchers have added a monofunctional compound to reduce the extent of conversion and hinder the onset of gelation.[26] It is also evident from Table 1 that TMA was a more effective branching agent than the trimethyl esters since there was a significantly higher gel fraction for the TMA branched polyesters at equivalent reaction conditions (99 and 56 wt % for TMA compared to 30 and 12 wt % for 1,3,5-TMT).

The degree of branching in the PET-*co*-PEI copolymers was quantified using the branching index value (g'), shown in eq 1

$$g' = \frac{[\eta]_{branched}}{[\eta]_{linear}} \tag{1}$$

where $[\eta]_{branched}$ and $[\eta]_{linear}$ are the intrinsic viscosities of branched and linear polymers of equivalent molecular weights. The g' values were determined using the procedure Hudson et al. reported, where a MALLS detector and a viscosity detector were coupled with the GPC column.[27] $[\eta]_{branched}$ was measured directly using the viscosity detector, and $[\eta]_{linear}$ was calculated using eq 2

$$[\eta]_{linear} = KM_w^{\ a} \tag{2}$$

where M_w of the branched PET-*co*-PEI was measured with the MALLS detector, and K (2.3×10^{-4}) and a (0.70) are the Mark−Houwink constants for linear PET-*co*-PEI generated from the viscosity detector.

Table 2 shows the intrinsic viscosities of the branched and linear PET-*co*-PEI and the branching index values. Since a branched chain has a higher segment density than a linear chain, a branched macromolecule occupies a smaller hydrodynamic volume than a linear polymer of equivalent molecular weight. Consequently, $g' = 1.0$

Table 2. Molecular Weight, Intrinsic Viscosity, and Branching Index Values for PET-*co*-PEI Series

branching agent	branching agent concn (mol %)	M_w (kg/mol)	M_w/M_n	$[\eta]_{branched}$ (dL/g)	$[\eta]_{linear}$ (dL/g)	g'
N/A[a]	0	11.7	1.4	0.17	0.16	1.02
N/A	0	77.3	1.6	0.55	0.58	0.95
1,3,5-TMT	0.5	49.2	3.7	0.34	0.43	0.80
1,2,4-TMT	0.5	106	2.5	0.55	0.78	0.70
TMA	0.5	94.0	2.9	0.53	0.84	0.63
1,3,5-TMT	3.0[b]	76.0	10.7	0.28	0.65	0.43

[a] N/A = not applicable. [b] Addition of 15 mol % dodecanol.

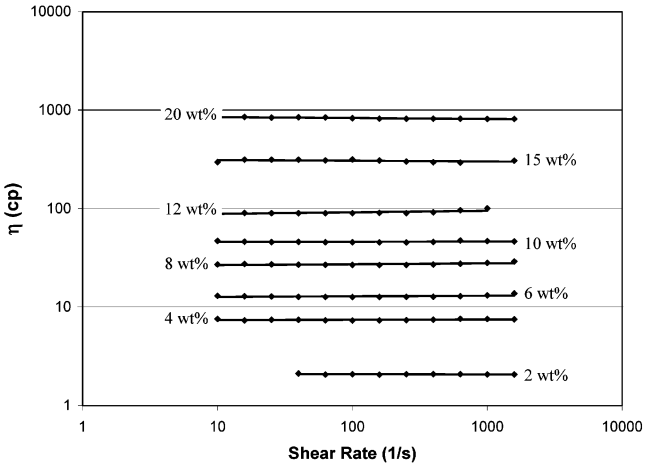

Figure 3. Dependence of viscosity on shear rate for linear PET-*co*-PEI (M_w = 77 300 g/mol) at various concentrations (2−20 wt % in 70/30 $CHCl_3$/DMF cosolvent).

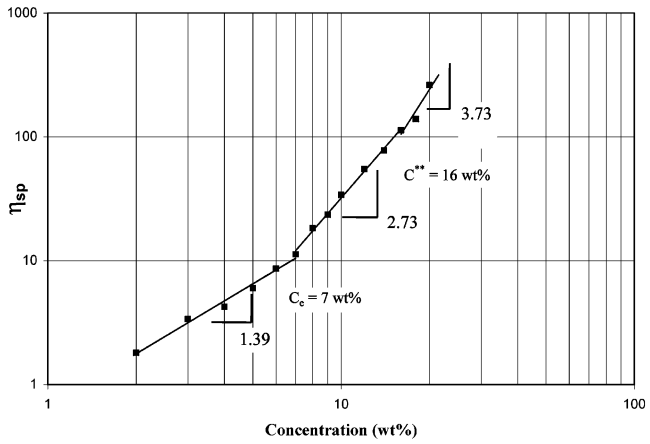

Figure 4. Dependence of specific viscosity on concentration for branched PET-*co*-PEI (M_w = 46 000 g/mol and g' = 0.8).

for a linear chain and g' decreases from 1.0 as the degree of branching increases.

As shown in Table 1, a significant gel fraction was observed for branching agent concentrations at 1.5 mol %. Consequently, to produce soluble, highly branched PET-*co*-PEI with 3 mol % of 1,3,5-TMT, the addition of a monofunctional compound (dodecanol) prevented network formation.[28] Table 2 depicts that the polymer with 3 mol % 1,3,5-TMT had a larger number of branches than the rest of the series based on the very broad molecular weight distribution (M_w/M_n = 10.7) and the low branching index value (g' = 0.43). Finally, it is again clear that TMA was a more effective branching agent than either 1,3,5-TMT or 1,2,4-TMT since employing 0.5 mol % of the TMA trifunctional compound resulted in a more highly branched polyester as seen from the branching index value (g' = 0.63 compared to g' = 0.80 and 0.70). The difference in the branching efficiency of the trifunctional compounds may be due to a disparity in the reactivity of the methyl ester vs the carboxylic acid and anhydride functional groups of TMT and TMA, respectively, toward the hydroxyl group of ethylene glycol. Future studies will address this hypothesis in more detail.

3.2. Solution Rheology and Determination of Concentration Regimes for Linear and Branched PET-*co*-PEI. The concentration regimes for the PET-*co*-PEI solutions were determined using solution rheology measurements. Shear rate sweeps from 80 to >1000 s^{-1} were performed on copolymer solutions ranging from 2 to >20 wt % in a 70/30 w/w $CHCl_3$/DMF cosolvent at 25 ± 0.2 °C. All polyester solutions showed Newtonian behavior over this range of shear rates; however, it should be noted that shear thinning will occur at higher shear rates. Figure 3 shows a plot of viscosity as a function of shear rate for a linear PET-*co*-PEI (M_w = 77 300 g/mol) at several different concentrations. The zero shear rate viscosity (η_0) increased from 2.1 to 820 cP as the concentration was increased from 2 to 20 wt %. The polymer contribution to the η_0 was studied by defining the specific viscosity (η_{sp}) in eq 3

$$\eta_{sp} = \frac{\eta_0 - \eta_s}{\eta_s} \tag{3}$$

where η_s is the solvent viscosity. For neutral, linear polymers in a good solvent, $\eta_{sp} \sim C^{1.0}$ in the dilute regime, $\eta_{sp} \sim C^{1.25}$ in the semidilute unentangled regime, $\eta_{sp} \sim C^{4.8}$ in the semidilute entangled regime, and $\eta_{sp} \sim C^{3.6}$ in the concentrated regime.[29] The η_{sp} is plotted as a function of concentration in Figure 4 for the branched PET-*co*-PEI (M_w = 49 200 g/mol and g' = 0.80). Changes in the slope marked the onset of the semidilute unentangled, semidilute entangled, and concentrated regimes. The entanglement concentration (C_e) and concentrated regime (C^{**}) were determined using the method employed by Colby et al.[17] C_e and C^{**} were found to be 7 and 16 wt %, respectively. The dilute region was not determined here since rheology was not performed on polymer solutions less than 2 wt %.

Figure 4 clearly shows that the semidilute unentangled regime $\eta_{sp} \sim C^{1.39}$ is in good agreement with the theoretical predictions (i.e., $\eta_{sp} \sim C^{1.25}$). In the semidilute entangled regime, the specific viscosity should scale with the polymer concentration to approximately the 4.8 power. However, a much weaker dependence was observed in the semidilute entangled regime ($\eta_{sp} \sim C^{2.7}$), which was attributed to the branched architecture of the PET-*co*-PEI copolymers. Finally, in the concentrated region, the concentration exponent was 3.7, in good agreement with the theoretical scaling law exponent of 3.8.

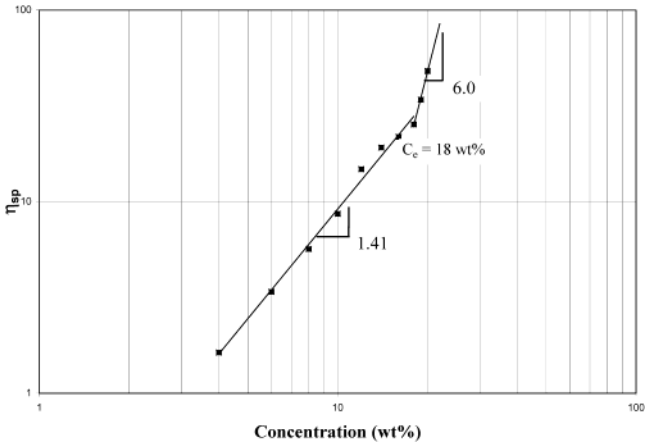

Figure 5. Dependence of specific viscosity on concentration for linear PET-*co*-PEI (M_w = 11 700 g/mol).

Table 3. C_e Values for Linear and Branched PET-*co*-PEI[a]

mol % branching agent	g'	M_w (kg/mol)	M_w/M_n	C_e (wt %)
0	1.02	11.7	1.6	18
0	0.95	54.2	1.7	6.0
0	0.99	77.3	1.6	4.5
0.5	0.80	49.2	2.4	7.0
0.5	0.73	106	2.8	5.0
0.5	0.63	94.0	2.9	5.5
3.0	0.43	76.0	10.7	10

[a] C_e increased as M_w decreased and g' decreased.

Figure 5 shows the concentration dependence of the η_{sp} for a linear PET-*co*-PEI copolymer with M_w = 11 700 g/mol. The change in slope from 1.4 to 6.0 at 18 wt % marked C_e, the boundary between the semidilute unentangled and semidilute entangled regimes. Similar analyses were performed for a series of linear and branched PET-*co*-PEI with varying levels of branching and molecular weights. The results are summarized in Table 3.

For the linear copolyesters (0 mol % branching agent), increasing M_w from 11 700 to 77 300 g/mol decreased the entanglement concentration from 18 to 4.5 wt % since the low molecular weight chains occupy a smaller hydrodynamic volume and require a higher concentration before they begin to topologically constrain one another and entangle. Table 3 indicates that branching has an influence on C_e. When comparing linear PET-*co*-PEI with a M_w of 77 300 g/mol and a branched copolymer (0.5 mol % branching agent) with a M_w of 94 000 g/mol and g' = 0.63, the branched polymer has a higher entanglement concentration despite a higher M_w. As the degree of branching was increased further to g' = 0.43 for the 76 000 g/mol PET-*co*-PEI (3 mol % branching agent), C_e increased to 10 wt %. This systematic increase in C_e was due to the higher segment density of the branched polymers and the branch points hindering chain overlap. Consequently, only the outermost chain ends can entangle with each other.[20]

3.3. Electrospinning of Branched PET-*co*-PEI. Linear and branched PET-*co*-PEI samples were electrospun from a 70/30 w/w $CHCl_3$/DMF cosolvent. PET-*co*-PEI was soluble in $CHCl_3$ at high concentrations; however, the high vapor pressure (159 kPa) of $CHCl_3$ caused rapid solvent evaporation during electrospinning that resulted in plugging of the syringe injection nozzle. DMF is less volatile than $CHCl_3$; however, the copolymer is not soluble in DMF at high concentrations.

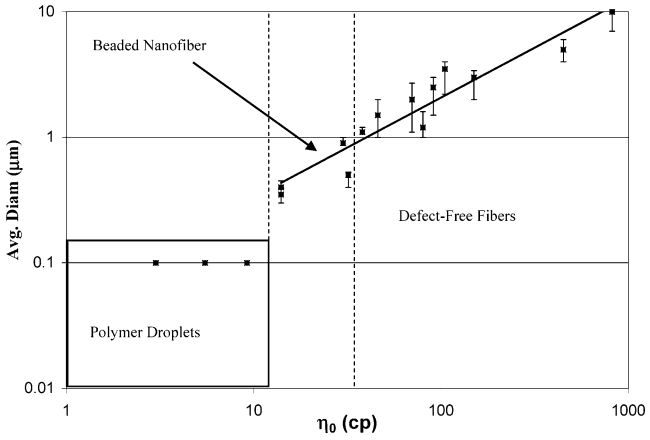

Figure 6. Dependence of electrospun fiber size on zero shear rate viscosity for linear and branched PET-*co*-PEI (R^2 = 0.91). Three distinct regimes of morphology were observed depending on η_0: polymer droplets, beaded nanofibers, and defect-free fibers.

Consequently, a mixed solvent of 70/30 w/w $CHCl_3$/DMF resulted in the desired solubility and volatility to facilitate electrospinning. Low levels of residual DMF were present in the electrospun fibers, while the presence of $CHCl_3$ was negligible. It should be noted that solution rheology and electrospinning conditions for the series of copolymers were identical (~25 °C and 70/30 w/w $CHCl_3$/DMF cosolvent), thereby ensuring the same hydrodynamic chain conformations in solution. The processing conditions were held constant to discern the effects of chain length and molecular topology on morphology of the electrospun fibers. Unless otherwise noted, all polymer solutions were electrospun at 18 kV potential, 3 mL/h flow rate from the syringe, and a 24 cm distance from the syringe tip to the grounded target. The polymers that were selected for electrospinning are listed in Table 3 and exhibit a broad range of molecular weights (11 700−106 000 g/mol) and degrees of branching (g' values of 1.0−0.43). As reported earlier, it was assumed the surface tensions of the solutions at various concentrations did not significantly change.[14,16]

The dependence of the electrospun fiber diameter on η_0 for the branched and linear PET-*co*-PEI is shown in Figure 6. Three distinct fiber morphologies were identified depending on the η_0 of the solution. Polymer solutions with a η_0 less than 10 cP produced polymer droplets when electrospun, while PET-*co*-PEI solutions with a η_0 between 10 and 30 cP generated fibers with beads as shown in Figure 6. Finally, electrospinning solutions with a η_0 greater than 30 cP yielded defect-free, uniform fibers. Moreover, the fiber diameter increased with η_0 by the relationship

$$\text{Diam} = 0.05[\eta_0]^{0.8} \quad (4)$$

where the fiber diameter is in microns. An increase in the zero shear rate viscosity indicated a larger number of entanglement couplings, thereby generating larger electrospun fibers.

Figure 7 shows FESEM images of fibers electrospun using 8−20 wt % solutions of branched PET-*co*-PEI (M_w of 76 000 g/mol and g' = 0.43). It should be noted that all FESEM images were taken at the same magnification. Table 3 illustrates that the C_e for the branched copolymer is 10 wt %. The fiber morphology was dependent on the concentration regime from which the

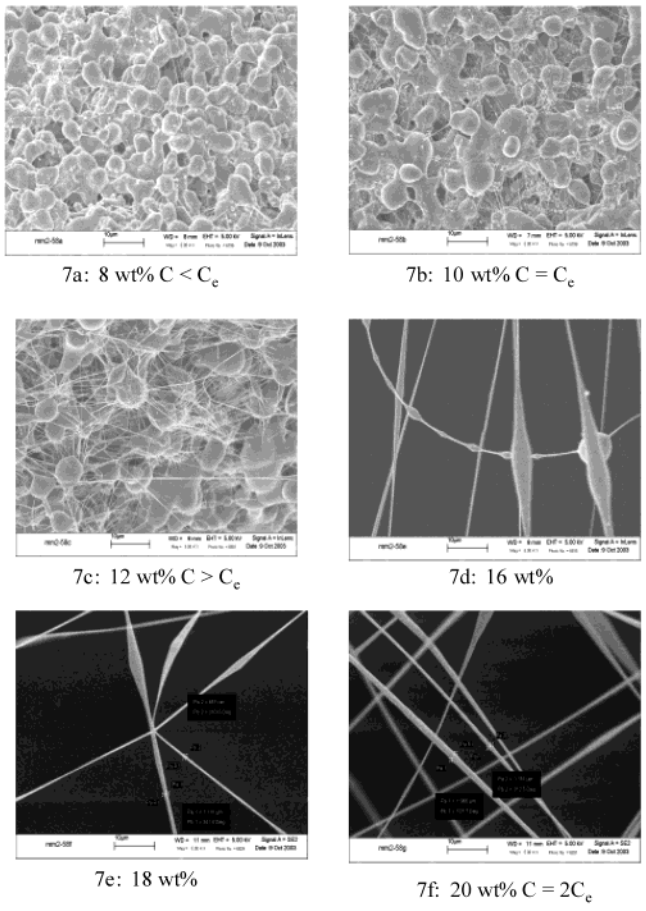

Figure 7. FESEM images of electrospun fibers of branched PET-*co*-PEI (M_w = 76 000 g/mol, g' = 0.43, C_e = 10 wt %) at several concentrations (8−20 wt %).

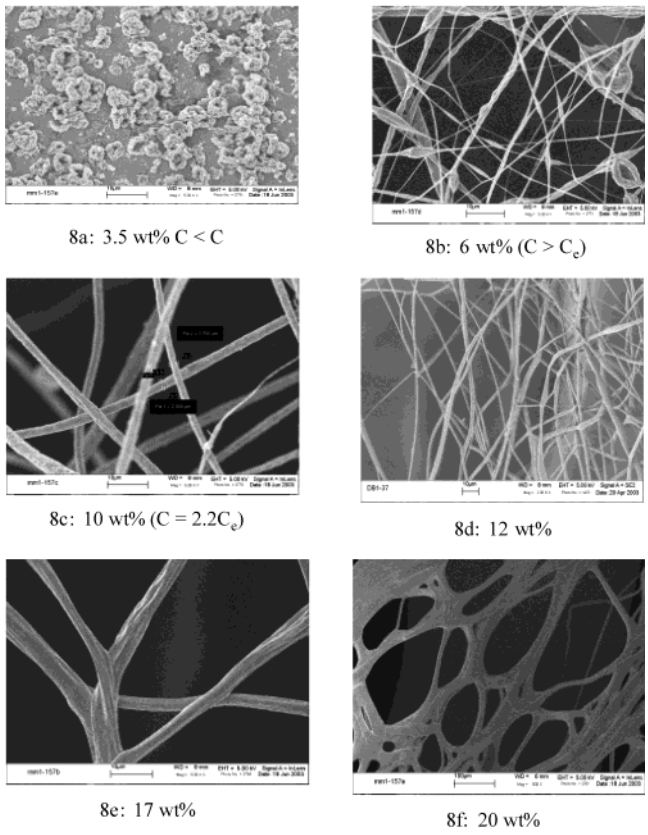

Figure 8. FESEM images of electrospun fibers of linear PET-*co*-PEI (M_w = 77 300 g/mol, C_e = 4.5 wt %) at several concentrations (3.5−20 wt %).

polymer was electrospun. In Figure 7a, it is clear that polymer solutions that were electrospun from solutions below the C_e of 10 wt % did not yield fibers, and only polymer droplets were observed. Since there is no topological constraint or entanglements between polymer chains in solutions below C_e, the jet could not withstand the surface tension of the solution or the force of the electric field and the jet broke up into droplets. When the concentration was raised to the C_e (10 wt %), fiber formation was observed between the polymer droplets (Figure 7b). As the concentration was raised beyond C_e, droplets and nanofibers were produced with an average fiber diameter of 0.25 μm (Figure 7c). For the 16 and 18 wt % solutions above C_e (10 wt %), beaded electrospun fibers were generated with diameters on the order of 0.70 and 0.90 μm, respectively (Figure 7d,e). It is important to note the change from predominately spherical beads to elongated bead in Figure 7d,e. This phenomenon was previously reported in the literature.[14] Above C_e, the high degree of chain overlap resulted in chain constraint and the formation of entanglement couplings. Figure 7f shows uniform, defect-free fibers with an average diameter of 1.2 μm from electrospinning a solution 2 times C_e. As the number of entanglements increased, the solution viscosity increased, thereby facilitating the formation of defect-free fibers.

Linear PET-*co*-PEI and branched PET-*co*-PEI of equivalent M_w exhibited similar behavior over the same concentration regimes. Figure 8 shows SEM images of a linear copolyester (M_w of 77 300 g/mol and C_e = 4.5 wt %). Below the C_e of 4.5 wt %, polymer droplets were primarily formed (Figure 8a). As the concentration was increased above C_e, beaded nanofibers were formed with average fiber diameters of 0.50 μm (Figure 8b). When the linear copolyester was electrospun from solutions above 2 times C_e (10 wt %), uniform, defect-free fibers were formed with average fiber diameters of 1.5 μm (Figure 8c). As the concentration was increased further to 12 and 17 wt %, uniform fibers with nominal diameters of 2.5 and 5 μm were respectively electrospun (Figure 8d,e). Attempts to electrospin 20 wt % solutions of the linear PET-*co*-PEI were unsuccessful unless the syringe pump flow rate was increased to 20 mL/h to overcome the high viscosity of the solution and initiate jet formation. This resulted in the formation of large fibers >10 μm in diameter (Figure 8f).

For the majority of copolymers listed in Table 3, C_e was the minimum concentration required for electrospinning of beaded nanofibers, while 2−2.5 times C_e was the minimum concentration required for electrospinning uniform, defect-free fibers. However, a different concentration dependence of fiber morphology was observed for the 11 700 g/mol linear PET-*co*-PEI (C_e = 18 wt %). It can be seen in Figure 9 that the concentration was increased well above C_e before beaded fibers were formed. Electrospinning from 18 and 20 wt % solutions both resulted in polymer droplets (Figure 9a,b). There was no presence of fibers until the concentration was raised to 20% above C_e (Figure 9c). Finally, electrospinning from 26 and 28 wt % solutions produce beaded nanofibers with nominal diameters of 0.20 and 0.40 μm, respectively (Figure 9d,e). Since 11 700 g/mol is not far above the critical molecular weight for entanglements of PET-*co*-PEI in the melt, it is more difficult for the low molecular weight chains to form entanglements,

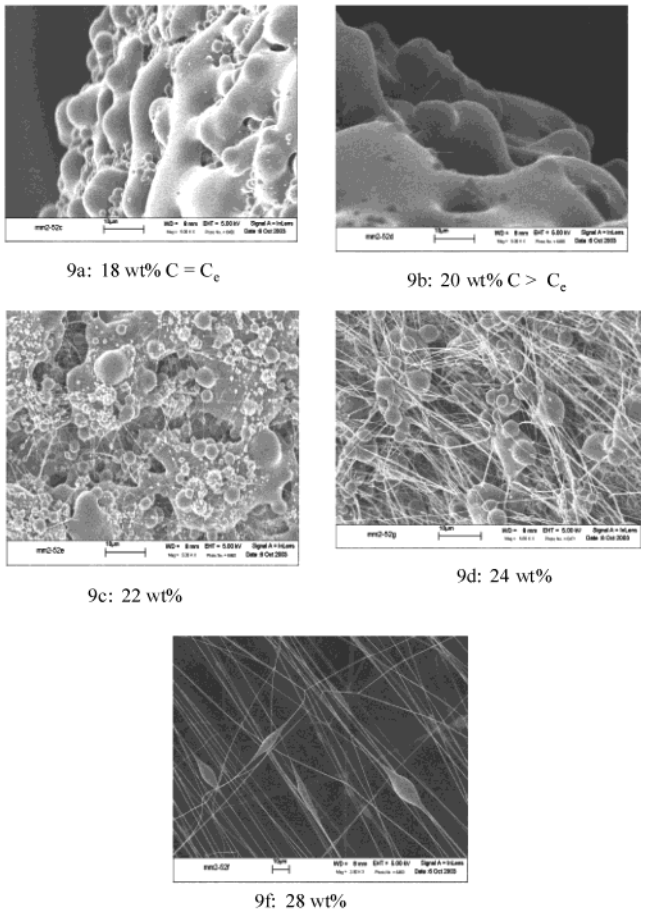

Figure 9. FESEM images of electrospun fibers of linear PET-*co*-PEI (M_w = 11 700 g/mol, g' = 0.8, C_e = 18 wt %) at several concentrations (18−28 wt %).

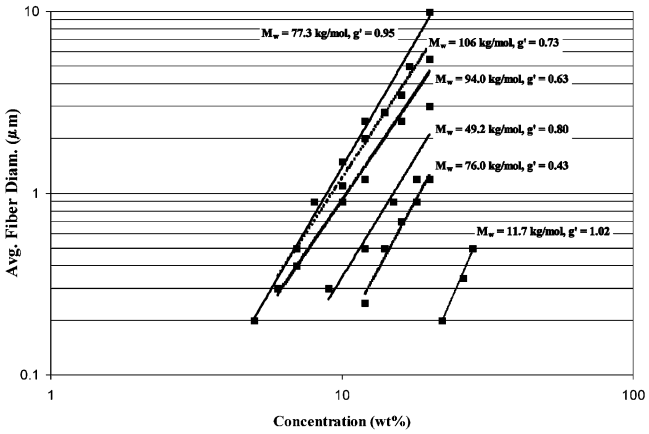

Figure 10. Dependence of fiber diameter on concentration for the series of linear and branched PET-*co*-PEI copolymers.

thereby favoring droplet formation or electrospraying.

The concentration dependence of the electrospun fiber diameter is summarized for the PET-*co*-PEI series in Figure 10. The diameter of the linear and branched PET-*co*-PEI fibers showed a ~3.0 power law dependence on solution concentration. The same power law relationship has been reported for other electrospun fiber systems.[30] In Figure 10, the intercept of each curve is different since the series covers a range of molar masses and degrees of branching. Consequently, to generate equivalent size fibers with this series of copolymers, the solution concentration was increased as the critical entanglement concentration of the respective polyester

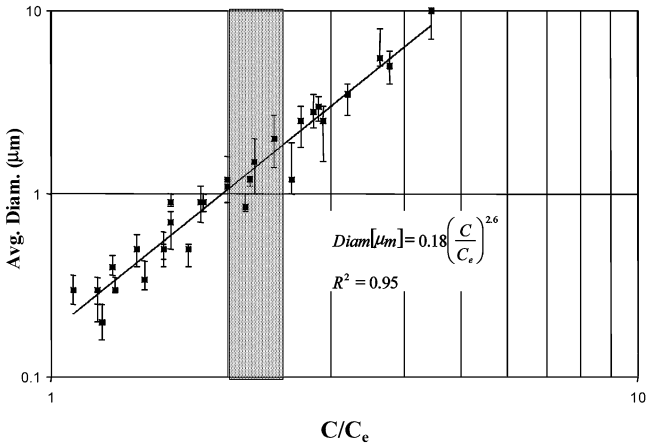

Figure 11. Dependence of fiber diameter on the normalized concentration for the PET-*co*-PEI series.

increased. For example, to produce fibers with an average diameter of 0.50 μm, the linear copolymers of M_w = 11 700 g/mol and M_w = 77 300 g/mol were electrospun from >28 and 7 wt % solutions, respectively, since the 11 700 g/mol copolyester possessed a C_e 4 times that of the 77 300 g/mol copolymer. Finally, in Figure 10, the fiber diameter vs concentration curve for the branched copolyesters was intermediate of the two linear copolymers since their entanglement concentrations were intermediate to those for the linear PET-*co*-PEI copolymers (see Table 3).

These curves in Figure 10 were superimposed when the solution concentration of each polyester were normalized with its respective C_e value. Figure 11 shows the superimposed curve for the dependence of fiber diameter on normalized solution concentration for the PET-*co*-PEI series, where the error bars represent the fiber size distribution. The influence of chain length and branching architecture on the electrospinning process was removed when the solution concentration was normalized with C_e. The fiber diameter scaled with the normalized concentration as

$$\text{Diam} \sim \left[\frac{C}{C_e}\right]^{2.6} \tag{5}$$

where C is the polymer concentration in solution and C_e the entanglement concentration. In Figure 11, the shaded region marks 2−2.5 times C_e, which was the minimum concentration required to electrospin high specific surface area, defect-free fibers. Equation 5 was predicted when a single equation was fit to the η_{sp} vs concentration data for the semidilute entangled and concentrated regions, predicting $C \sim \eta_{sp}^{3.3}$. When this relationship was substituted into eq 4, it was predicted that Diam $\sim C^{2.6}$, which is identical to the scaling argument in eq 5. Future work will address the sensitivity of the relationship in eq 5 to process parameters, including volumetric flow rate and electric field strength.

4. Conclusions

The implications of the semidilute unentangled and semidilute entangled concentration regimes on the electrospinning process were determined for a series of linear and branched PET-*co*-PEI copolymers. Branching index and gel fractions revealed differences in branch

structure depending on the branching agent used. In particular, polyesters polymerized in the presence of TMA showed more highly branched topologies compared to those polymerized with 1,3,5-TMT or 1,2,4-TMT. Analyzing the dependence of specific viscosity (η_{sp}) on concentration enabled the determination of the semidilute unentangled, semidilute entangled, and concentrated regimes for the PET-*co*-PEI solutions. For equivalent molecular weights, C_e increased with branching due to the higher segment density of the branched polymers and the branch points hindering chain overlap and entanglement.

Linear and branched copolymers were then electrospun from the semidilute unentangled and semidilute entangled regions to determine the effects of concentration regime and molecular topology on electrospun fiber morphology. Fiber morphology was dependent on the zero shear rate viscosity, with the presence of three distinct morphology regimes: polymer droplets, beaded nanofibers, and uniform, defect-free fibers. Moreover, the fiber diameter scaled with the η_0 to the 0.8 power. For most of the copolymers studied, C_e was the minimum concentration required for electrospinning of beaded nanofibers, while 2−2.5 times C_e was the minimum concentration required for electrospinning uniform, defect-free fibers. Low molecular weight (M_w = 11 700 g/mol), linear PET-*co*-PEI required $C > C_e$ to form beaded fibers since this is not far above the critical molecular weight for entanglements of PET-*co*-PEI in the melt. When the concentration was normalized using C_e, the influence of chain length and branching architecture on the electrospinning process was removed, and the fiber diameter universally scaled with the normalized concentration to the 2.6 power.

Acknowledgment. This material is based upon work supported by the U.S. Army Research Laboratory and U.S. Army Research Office under Grant DAAD19-02-1-0275 Macromolecular Architecture for Performance (MAP) MURI. The authors also thank Eastman Chemical Co. for their continued support of polyester research in supporting areas. Mr. Pankaj Gupta in the Department of Chemical Engineering at Virginia Tech and Professor Gary Wnek at Virginia Commonwealth University are acknowledged for their assistance in the electrospinning setup.

References and Notes

(1) Reneker, D. H.; Chun, I. *Nanotechnology* **1996**, *7*, 216.
(2) Deitzel, J. M.; Kleinmeyer, D.; Harris, D.; Beck Tan, N. C. *Polymer* **2001**, *42*, 261.
(3) Taylor, G. I. *Proc. R. Soc. London, Ser. A* **1969**, *313*, 453.
(4) Reneker, D. H.; Yarin, A. L.; Fong, H.; Koombhongse, S. *J. Appl. Phys.* **2000**, *87*, 4531.
(5) Hohman, M. M.; Shin, M.; Rutledge, G.; Brenner, M. P. *Phys. Fluids* **2001**, *13*, 2201.
(6) Shin, Y. M.; Hohman, M. M.; Brenner, M. P.; Rutledge, G. C. *Polymer* **2001**, *42*, 9955.
(7) Deitzel, J. M.; Kosik, W.; McKnight, S. H.; Beck Tan, N. C.; Desimone, J. M.; Crette, S. *Polymer* **2002**, *43*, 1025.
(8) Grafe, T.; Graham, K. *Nonwoven Technol. Rev.* **2003**, 51.
(9) Kenawy, E.-R.; Layman, J. M.; Watkins, J. R.; Bowlin, G. L.; Matthews, J. A.; Simpson, D. G.; Wnek, G. E. *Biomaterials* **2003**, *24*, 907.
(10) Matthews J. A.; Wnek, G. W.; Simpson, D. G.; Bowlin, G. L. *Biomacromolecules* **2002**, *3*, 232.
(11) Gupta, P.; Wilkes, G. L. *Polymer* **2003**, 6353.
(12) Megelski, S.; Stephens, J. S.; Chase, D. B.; Rabolt, J. F. *Macromolecules* **2002**, *35*, 8456.
(13) Lee, K. H.; Kim, H. Y.; La, Y. M.; Lee, D. R.; Sung, N. H. *J. Polym. Sci., Part B: Polym. Phys.* **2002**, *40*, 2259.
(14) Fong, H.; Chun, I.; Reneker, D. H. *Polymer* **1999**, *40*, 4585.
(15) Zong, X.; Kim, K.; Fang, D.; Ran, S.; Hsiao, B. S.; Chu, B. *Polymer* **2002**, *43*, 4403.
(16) Jun, Z.; Hou, H.; Schaper, A.; Wendroff, J. H.; Grenier, A. *e-Polym.* **2003**, *009*, 1.
(17) Colby, R. H.; Fetters, L. J.; Funk, W. G.; Graessley, W. W. *Macromolecules* **1991**, *24*, 3873.
(18) Krause, W. E.; Bellomo, E. G.; Colby, R. H. *Biomacromolecules* **2001**, *2*, 65.
(19) Graessley, W. W. *Polymer* **1980**, *21*, 258.
(20) Burchard, W. *Adv. Polym. Sci.* **1999**, *143*, 114.
(21) Lin, Q.; Unal, S.; Fornof, A. R.; Yuping, W.; Li, H.; Arementrout, S. R.; Long, T. E. *Macromol. Symp.* **2003**, *199*, 163.
(22) Kang, H.; Lin, Q.; Armentrout, S. R.; Long, T. E. *Macromolecules* **2002**, *35*, 8738.
(23) Lin, Q.; Pasatta, J.; Wang, Z.-H.; Ratta, V.; Wilkes, G. L.; Long, T. E. *Polym. Int.* **2002**, *51*, 540.
(24) Ramakrishnan, S.; Jayakannan, M. J. *J. Polym. Sci., Part A: Polym. Chem.* **1998**, *36*, 309.
(25) Chen, L.-W.; Chen, J.-W. *J. Appl. Polym. Sci.* **2000**, *75*, 1221.
(26) Manaresi, P.; Munari, A.; Pilati, F.; Alfonso, G. C.; Russo, S.; Sartirana, L. *Polymer* **1986**, *27*, 955.
(27) Hudson, N.; MacDonald, W. A.; Neilson, A.; Richards, R. W.; Sherrington, D. C. *Macromolecules* **2000**, *33*, 9255.
(28) Flory, P. J. *Principles of Polymer Chemistry*; Cornell University Press: Ithaca, NY, 1953.
(29) de Gennes, P. G. *Scaling Concepts in Polymer Physics*; Cornell University Press: Ithaca, NY, 1979.
(30) Demir, M. M.; Yilgor, I.; Yilgor, E.; Erman, B. *Polymer* **2002**, *43*, 3303.

MA035689H